paper. In other words, in the heptamers the dipole moment arising from the central disk is weaker as compared to collective opposite mode resulting from the six outer disks. But in this work, it is found that when the number of outer disks is reduced from six to four, the ratio value between two collective opposite modes increases. It is a result of changing the ratio between the opposing phase oscillating plasmons from 1/6 in the heptamers to 2/3 in the pentamers as shown in Fig. 2(e). The FR can be seen obviously in the experimental spectra in Fig. 2(b). It can promote the efficiency of biological and chemical detection [1].

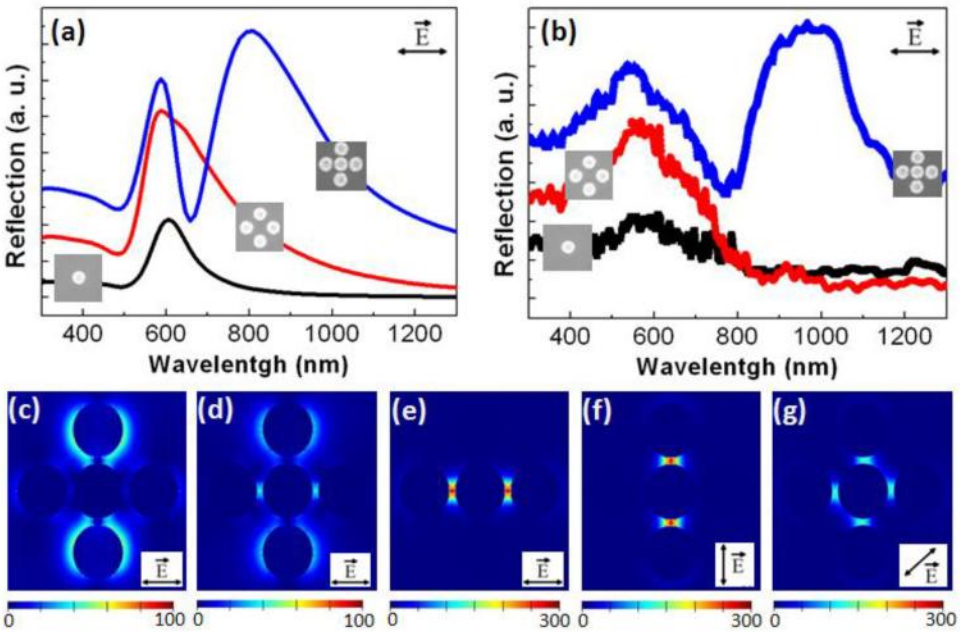

Fig. 3. (a) Simulated and (b) experimental reflection spectra of the monomers, quadrumers and pentamers at x-polarized normal incidence. Calculated field distribution at x-polarized normal incidence at the wavelengths of (c) 585 nm, (d) 670 nm and (e) 805 nm and at a wavelength of 805 nm and at (f) y-polarized and (g) 45-degree polarized light incidence.

For our fabricated pentamers, pronounced Fano-minimum can be observed in reflection responses as well. To measure the reflection mode, the arrays of monomers, quadrumers and pentamers of the same sizes and configuration were fabricated on the silicon substrates. Figures 3(a) and (b) show the reflection spectra of these structures by simulation and experiment, respectively. The presence of the collective dipolar plasmon resonances in the monomers and quadrumers are the same as those shown in the transmission spectra in Fig. 2. Meanwhile, the Fano-line shape can be seen in the pentamer reflection spectrum as well. Figure 3 reveals that the reflection results also possess a good qualitative agreement with the simulated results. In order to elucidate the character of the resonances, electric field distributions for the Au pentamers in various wavelengths are shown in Figs. 3(c) to (g). Distribution of field intensity corresponding to the collective dipolar moments is plotted in Figs. 3(c) and (e) at 585 nm and 805 nm, respectively. The field distribution corresponding to the maximum destructive interferences of the sub-radiant and super-radiant modes can be seen in Fig. 3(d) at 670 nm, where the effect of destructive interference on the value of both dipolar moments leads to the emergence of Fano line-shape in the reflection spectrum. An interesting feature in this design is its unique spatial electric field distribution and light amplification. Figure 3(e) shows how the pentamer is able to concentrate light down to sub-20 nm gaps at the wavelength of 805 nm. This plot displays the local field intensity redistribution within the gaps among the central disk and disks A and C of the pentamer at x-polarized

#140227 - $15.00 USD Received 3 Jan 2011; revised 28 Jan 2011; accepted 12 Feb 2011; published 1 Mar 2011

illumination. The field intensity shows hundreds-fold increase only inside the gaps which reveals that these separated disks can be used as an optical antenna. Meanwhile, Figs. 3(f) and (g) show the pentamer structures at y-polarized and 45 degree-polarization (in X-Y plane) illumination, respectively. These plots demonstrate that the field can be strongly localized in the left and right gaps under x-polarized excitation, but in the top and bottom gaps under y-polarized excitation and in these four gaps under a 45-degree polarization. It is the unique feature of the pentamers to store light energy in different positions selectively by changing the polarization. Keeping in mind that the total amount of re-distributed field intensities which are shown in Figs. 3 (c) to (g) kept constant during changing the polarization orientation. For spatial control over the nanoscopic field distribution, this structure does not require co-illumination by two light sources [11] and the adjustment of the phase delay between them [11, 17]. This advantage benefits potential applications for plasmon-based all optical information processing [11] and control of light matter interactions in the nanoscales [24].

Optical responses of the pentamers can be explained by a spring-mass model [6, 25] which consists of five coupled interacting oscillators illustrated in Fig. 4(a). According to the field distribution plots in Figs. 3(c) to (g), two hypotheses are argued. Firstly, the springs among the outer disks in the oscillator system are neglected since the outer disks in the pentamers do not have considerable interactions between each other. This can be inferred from the transmission spectra of the quadrumers in Fig. 2 where a dipole resonance identical to the monomer is seen. Secondly, the interacting system of the five coupled oscillators can be simplified to a three coupled interacting oscillators system, because the coupling among disks A and C with respect to disk E are similar, as well as disks B and D with respect to disk E. Figure 4(b) displays the simplified system in which mass 1 represents disk E, mass 2 represents disks A and C, and mass 3 represents disks B and D. This model is an extension of the classical two oscillators system which was used to study the nature of FR [6] and three oscillator system as the analogous of Fano-shell structures [8]. In Fano-shell model, all three oscillators are connected to each other because of direct effect of dipole, quadrupole and dark modes on each other, under optical excitation. But in the model presented in this work the spring between oscillators 2 & 3 are neglected since the interaction of ring-like disks in pentamers are neglectable and each of surrounding disks just approach the central disk individually and directly during optical excitation.

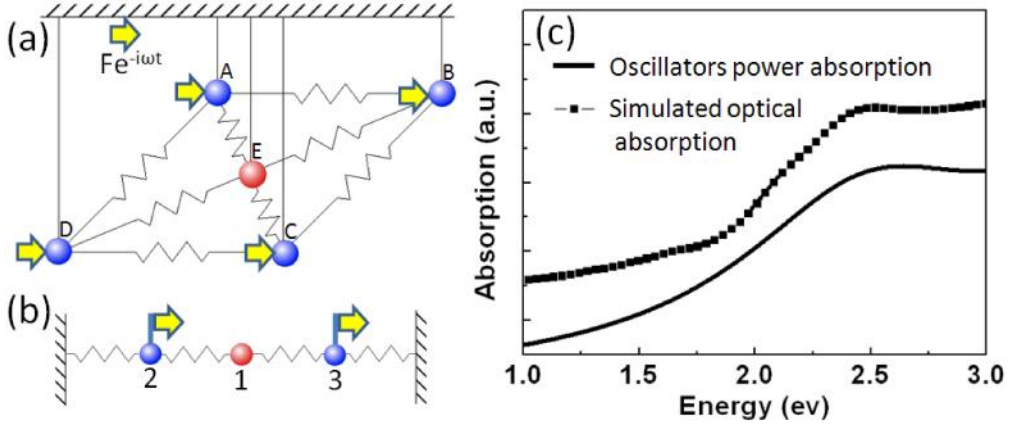

Fig. 4. (a) Five coupled interacting oscillators representing the pentamer optical responses, (b) simplified three coupled oscillators and (c) simulated plasmons absorption spectra by FDTD (dot line) and calculated power absorption in the oscillator model (solid line).

The mass values in this model are assumed as $m_1=m_2=m_3=1$ and all springs are the same. As explained before, the dark mode is a result of adding the central disk. Therefore outer oscillators are taken to be driven by a harmonic force $\mathbf{F}(t)= \mathbf{F}e^{-i\omega t}$ as the bright mode

#140227 - $15.00 USD Received 3 Jan 2011; revised 28 Jan 2011; accepted 12 Feb 2011; published 1 Mar 2011

exhibitors. Subsequently, in the simplified system the oscillators 2 and 3 are taken to be driven by a harmonic force. It is unlike to Fano-shell mechanical model [8] in which the dipole bright mode is assumed as the responsible for exciting the quadrupolar mode and subsequently sub-radiant dark mode and only one oscillator is driven by harmonic force. For coupled oscillators model in this work, the motion equations of oscillators |1>, |2> and |3> are solved in terms of displacements x_1, x_2 and x_3 from the equilibrium positions:

$$\ddot{x}_1(t) + \gamma_1 \dot{x}_1(t) + \omega_1^2 x_1(t) - \Omega^2 x_2(t) - \Omega^2 x_3(t) = 0, \quad (1)$$

$$\ddot{x}_2(t) + \gamma_2 \dot{x}_2(t) + \omega_2^2 x_2(t) - \Omega^2 x_1(t) = Fe^{-i\omega t}, \quad (2)$$

$$\ddot{x}_3(t) + \gamma_3 \dot{x}_3(t) + \omega_3^2 x_3(t) - \Omega^2 x_1(t) = Fe^{-i\omega t}, \quad (3)$$

where $\boldsymbol{\omega_1}$, $\boldsymbol{\omega_2}$ and $\boldsymbol{\omega_3}$ are oscillation frequencies, corresponding to the oscillators 1, 2, and 3, respectively, and $\boldsymbol{\Omega}$ coherent coupling frequencies between interconnected oscillators which represents the coupling between anti-parallel modes in the optical system. $\boldsymbol{\gamma_1}$, $\boldsymbol{\gamma_2}$ and $\boldsymbol{\gamma_3}$ are the friction coefficients which are used to account for the energy dissipation of |1>, |2> and |3>, respectively. These friction coefficients represent the dissipated energy among nano-disks during energy transformation at optical excitation. By tuning the coupling between bright mode and dark mode ($\boldsymbol{\Omega^2}$=1.69) and other parameters ($\boldsymbol{\omega_1}$ =2.5 eV, $\boldsymbol{\omega_2}$ =3.1 eV, $\boldsymbol{\omega_3}$ =5 eV, $\boldsymbol{\gamma_1}$=1, **@003@004@005** $\boldsymbol{\gamma_2}$ **@003@005**=42E-2, $\boldsymbol{\gamma_3}$ =20E-2 and F=10), the absorption power of the oscillator system reproduces the optical absorption of the pentamer. Figure 4(c) shows the comparison between absorbed powers of the oscillator system calculated by Eqs. (1) to (3) with the FDTD simulated plasmon response of the pentamer. As it was seen in Figs. 2(a) and 3(a), in pentamers the reflection and the transmission spectra posses almost a reverse trend. Consequently the absorption spectrum does not experience a pronounced peak as can be seen in Fig. 4(c). However it keeps increasing with the rise of the energy. The trend which is almost reproduced by absorption response of the classical oscillators model.

Conclusions

In summary, a five same nano-disk pentamer exhibiting a high contrast FR is investigated. The FR was obtained under normal incident light along all orientations of polarization. It was demonstrated that the monomers and the ring-like quadrumers behave the same as the isolated nano-disks exhibiting only the isolated mode. After the addition of the central disk into the center of the quadrumers to form the pentamers, an anti-parallel coupling of dipolar modes appears. The ratio between anti-parallel and parallel dipole modes is 2/3 and results in the generation of a pronounced FR as compared to the other planar symmetric structures. The existence of a FR in the pentamers was explained by the mass-spring oscillator model. Meanwhile, the polarization orientation is found to be an efficient tool to tune the localization of the electromagnetic intensity in nanoscales. It was shown that the pentamer can manipulate light in a sub-diffraction length scale and overcome the spatial restrictions of conventional optics. The tuning of light spatial distribution can be achieved by only a single source, instead of applying a phase shift in a co-illumination system.

Acknowledgements

The authors would like to acknowledge the funding provided by SERC Agency of Science, Technology And Research (A*STAR) Superlens Program (Project No. 092 154 0099) for the research work published in this paper. In addition the authors thank Professor Stefan A. Maier and Dr. Dang Yuan Lei for useful discussion and comments. Mohsen Rahmani would like to express his gratitude for the support from the A*STAR – SINGA scholarship program.

#140227 - $15.00 USD Received 3 Jan 2011; revised 28 Jan 2011; accepted 12 Feb 2011; published 1 Mar 2011